

## Interface-driven magnetocapacitance in a broad range of materials

This article has been downloaded from IOPscience. Please scroll down to see the full text article.

2008 J. Phys.: Condens. Matter 20 322202

(<http://iopscience.iop.org/0953-8984/20/32/322202>)

View [the table of contents for this issue](#), or go to the [journal homepage](#) for more

Download details:

IP Address: 129.252.86.83

The article was downloaded on 29/05/2010 at 13:47

Please note that [terms and conditions apply](#).

## FAST TRACK COMMUNICATION

# Interface-driven magnetocapacitance in a broad range of materials

Mario Maglione

ICMCB-CNRS, Université de Bordeaux, 87 Av Dr Schweitzer, F-33806 Pessac, France

E-mail: [maglione@icmcb-bordeaux.cnrs.fr](mailto:maglione@icmcb-bordeaux.cnrs.fr)

Received 23 April 2008, in final form 23 June 2008

Published 18 July 2008

Online at [stacks.iop.org/JPhysCM/20/322202](http://stacks.iop.org/JPhysCM/20/322202)

## Abstract

Triggered by the revival of multiferroic materials, a lot of effort is presently underway to find a coupling between a capacitance and a magnetic field. We show in this paper that interfaces are the right way of increasing such a coupling provided free charges are localized on these two-dimensional defects. Starting from commercial diodes at room temperature and going to grain boundaries in giant permittivity materials and to ferroelectric domain walls, a clear magnetocapacitance is reported which is all the time more than a few per cent for a magnetic field of 90 kOe. The only tuning parameter for such strong coupling to arise is the dielectric relaxation time which is reached on tuning the operating frequency and the temperature in many different materials.

(Some figures in this article are in colour only in the electronic version)

Following the ‘revival’ of multiferroic materials [1], many research groups are looking for a coupling between a magnetic field and the dielectric permittivity of materials. Not only applications but also reaching a basic understanding is the driving force for such an extended effort. Since the number of materials which display simultaneously ferroelectric polarization and magnetic order at room temperature is rather limited [2, 3], one is looking for alternative routes. More specifically, concerning the magnetocapacitance, a direct room temperature coupling of an external magnetic field with microscopic polarizabilities is still to be found. This is why integrated [4] and bulk [5] composites have been designed so as to increase the density of interfaces between ferroelectric and ferromagnetic materials. In piezoelectric-based devices, the generation of an ac current at the piezoresonance is readily achieved [6]. Very recently this effect, driven by elastic deformation, has been found in very standard multilayer ceramic capacitors [7], which opens up a broad range of applications. Nonetheless room temperature magnetocapacitance, i.e. the change of a capacitance by a magnetic field, is still an open question. Recently, Catalan has shown that nonlinear resistance at interfaces can be the right way to find such an effective coupling [8]. In this paper, we apply this concept to several very different materials. In

a first step, we recall that nonlinear resistance of diodes is of everyday use in sensing magnetic fields. In the blocking regime, it is thus very easy to observe room temperature 15% magnetocapacitance in one-cent diodes provided the operating frequency is set to the right range. We will then move to so-called ‘giant permittivity’ materials [9–12] which include charged interfaces [13–15]. Setting the temperature to the right range a magnetocapacitance is observed in the case of  $\text{CaCu}_3\text{Ti}_4\text{O}_{12}$ , an archetype of giant permittivity materials. Finally, we focus on more mesoscopic interfaces which are charged ferroelectric domains walls in Fe-doped  $\text{BaTiO}_3$ . A magnetocapacitance is clearly seen in the temperature and frequency range where the domain walls are relaxing. With this collection of results from many different materials we demonstrate that effective magnetocapacitance is a very general trend in charged interface materials.

The samples were inserted in a Quantum Design PPMS set up at the end of a modified holder using four coaxial cables linked to an HP4194 impedance analyzer through BNC connectors and cables. The samples were held freely by two soft wires at the center of the superconducting coil to avoid any spurious strain contributions. For fixed temperature runs, the impedance was recorded at given time intervals in the frequency range 1 kHz–1 MHz while the magnetic field

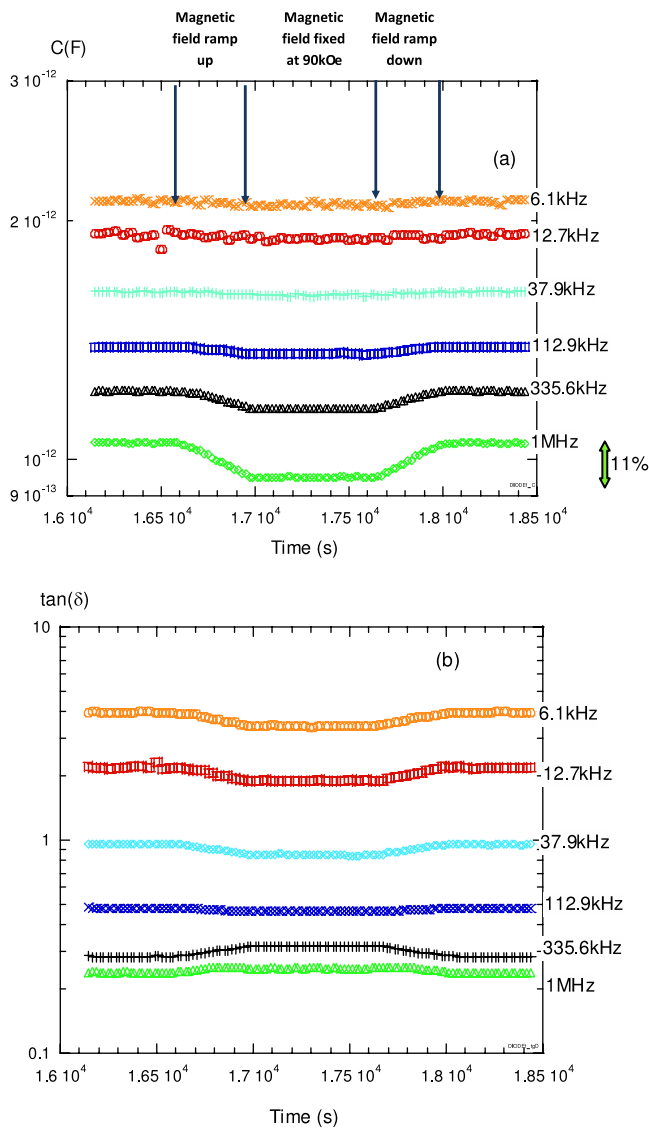


**Figure 1.** Room temperature capacitance (a) and dielectric losses (b) of a commercial diode in the blocking regime at several frequencies versus time. The slopes and central dwell time mark the magnetic field ramping and stabilization, respectively. The maximum magnetocapacitance is 15% for  $H = 90$  kOe at  $f = 1$  MHz.

was raised at a rate of  $200 \text{ Oe s}^{-1}$  from 0 to 90 kOe and then reduced back to 0 after a stabilization dwell time at the maximum field. Such a magnetic field run is sketched by arrows in figure 1(a). For temperature experiments, the magnetic field was fixed while the sample temperature was swept at a rate of  $0.1 \text{ K min}^{-1}$  up to  $1 \text{ K min}^{-1}$  and the sample impedance recorded at several spot frequencies.

Before describing the main part of our experimental result, we should make a point as to the technical observation of magnetocapacitance. Indeed, the application of a strong magnetic field to dielectric cells needs some caution. In very standard equipment, we have observed a temperature change of 0.01 K when the magnetic field was raised from 0 to 90 kOe. Even though small, such an electronic disturbance may lead to artificial magnetocapacitance, all the more serious in temperature ranges where the sample's

dielectric parameter changes very quickly against temperature. For example we have probed ferroelectric samples which include neither any magnetic component nor do they have charged interfaces. High purity potassium tantalate was one of these which undergoes a strong divergence of its dielectric permittivity at  $T < 100$  K. Under isothermal conditions we achieved artificial magnetocapacitance of several per cent which, using a differentiation process, could be ascribed to temperature fluctuations of about 0.01 K. This will thus be taken as the resolution limit in the following: if the observed magnetocapacitance at a given temperature could stem from a 0.01 K fluctuation, it will simply be discarded.

We now start with the first example which is again not new but which will fix the experimental conditions for the following. First, care was taken so as to keep the diode in its blocking regime. In this case, the equivalent circuit of the diode is a capacitor with a given level of losses. In figure 1, we plotted the capacitance and the dielectric losses versus time at several spot frequencies; the magnetic field run is sketched in figure 1(a). In a way which is shifted versus frequency  $f$ , a change of capacitance  $\Delta C(f)/C(f) = (C(90 \text{ kOe}, f) - C(0 \text{ Oe}, f))/C(0 \text{ Oe}, f)$ , which we will call magnetocapacitance in the following, is observed. The maximum magnetocapacitance is about  $-11\%$  for  $f = 1$  MHz. The dispersion of  $\Delta C(f)/C(f)$  versus frequency is a signature of the dispersive behavior of the diode capacitance. The dielectric losses  $\tan(\delta)$  also experience more than 10% variation under 90 kOe, also depending on the operating frequency. Both the magnetocapacitance and the dielectric losses' variations may be ascribed to the conducting charges in the semiconductors. Interface charges are dynamically recombining at the p-n interfaces and the external magnetic field, which changes the free charge trajectories through the Hall effect, alters the dynamical capacitance [16]. Indeed, the Lorentz force on the p and n carriers leads to a common bending of these carriers because of their alternating charge and trajectories. As a consequence, recombination of free carriers is favored and the space charge localization is decreased. Translated into terms of capacitance in the blocking regime, a decrease of space charge accumulation results in a decrease of  $C$  and that is what was observed in figure 1(a). Obviously, because a commercially available diode was used for the sake of generality, more elaborate structures should be designed in order to get a more comprehensive insight into such an effect. The diode magnetocapacitance may thus be described as resulting from the interaction of the external magnetic field with the free charges accumulated at the p-n interface.

Next, we turn to materials where interfaces are much less defined than in p-n junctions. In  $\text{CaCu}_3\text{Ti}_4\text{O}_{12}$  ceramics, a balance between the inner grain conductivity and grain boundary barriers is the source of an effective giant permittivity [13]. The very specific feature of this huge permittivity is that it is frequency- and temperature-independent at room temperature while it relaxes following a Debye-type behavior at low temperatures [9]. In these ceramics, we performed a magnetocapacitance experiment at room temperature without any sign of coupling in the

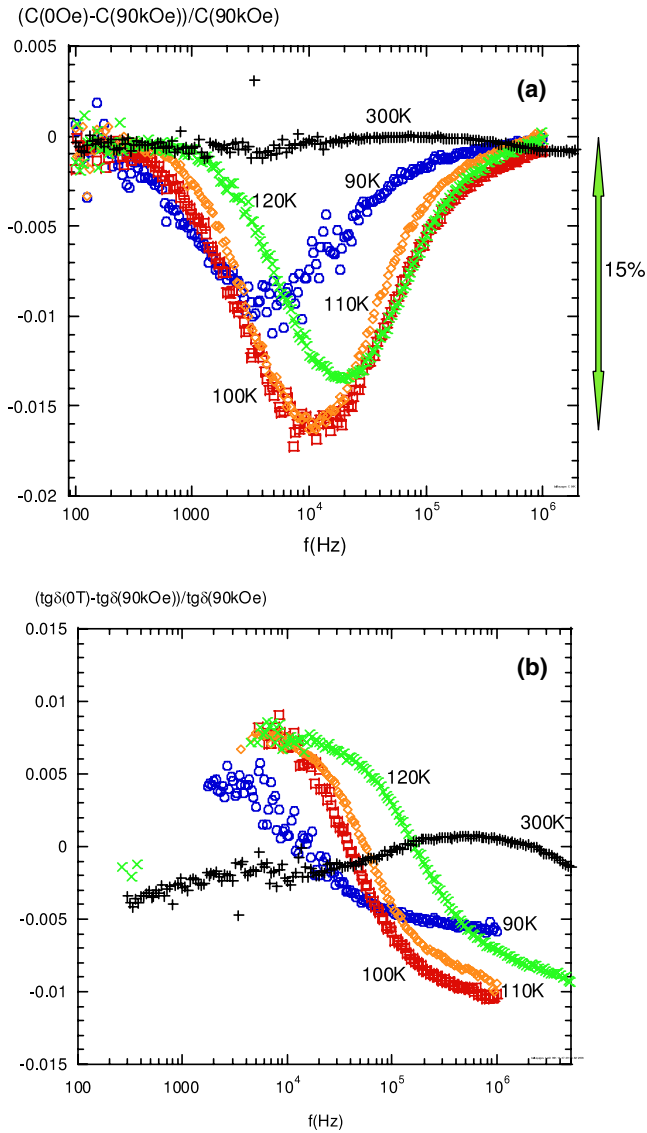


**Figure 2.** Relative variation under a magnetic field of 90 kOe of the capacitance (a) and dielectric losses (b) of a  $\text{CaCu}_3\text{Ti}_4\text{O}_{12}$  ceramic in the temperature range of its dielectric relaxation. The maximum of magnetocapacitance, which can be up to 15%, follows the dielectric relaxation frequency which increases when the temperature is raised. At room temperature  $T = 300$  K no magnetocapacitance is found.

limit of the above-mentioned temperature fluctuation. When, however, the sample temperature was fixed in the relaxation range of 100 K, a magnetocapacitance  $\Delta C(f)/C(f)$  is recorded (figure 2(a)). At all temperatures, a maximum magnetocapacitance is observed whose frequency increases with temperature exactly in the same way as the relaxation frequency. At the same time, the dielectric losses  $\tan \delta$  displayed a variation  $\Delta \tan \delta(f)/\tan \delta(f)$  evolving as an S-shaped curve on increasing the operating frequency (figure 2(b)). This is nothing other than the Kramers–Kronig transform of the  $\Delta C(f)/C(f)$  curves of figure 2(a). To exclude the possible thermal fluctuation as the source of these variations, we simulated a temperature variation of 0.01 K and found  $\Delta C(f)/C(f)$  and  $\Delta \tan \delta(f)/\tan \delta(f)$  at least 10 times smaller than the one plotted in figure 2.

Temperature fluctuations are thus not the origin of the observed magnetocapacitance. We thus conclude that the magnetocapacitance in  $\text{CaCu}_3\text{Ti}_4\text{O}_{12}$  ceramics is observable in the temperature and frequency range of their dielectric relaxation. Since this dielectric relaxation was ascribed to a grain boundary layer acting as a dielectric barrier between the conducting grains [13], we propose that the magnetocapacitance originates from a similar process as in the diode. Free charges accumulated at the grain boundary barrier are interacting with the magnetic field. Since dielectric relaxation is observed when the temperature and frequency are tuned so as to probe the dynamical motion of these charges among these interfaces, the magnetocapacitance is maximal right at the dielectric relaxation. We note that a similar magnetocapacitance at the relaxation frequency was already reported in  $\text{LuFe}_2\text{O}_4$ , another example of effective giant permittivity material [14]. Since this material also belongs to the broad family of grain-boundary layer dielectrics [15], a similar magnetocapacitance as in  $\text{CaCu}_3\text{Ti}_4\text{O}_{12}$  is not a surprise. We suggest here a model for this magnetocapacitance in  $\text{CaCu}_3\text{Ti}_4\text{O}_{12}$  ceramics. Within the model of Catalan [8], the observed magnetocapacitance needs a magnetoresistive part whose nonlinear behavior translates in capacitance through an appropriate equivalent circuit. We, however, need to go beyond this model to explain why the maximum magnetocapacitance is observed right at the relaxation frequency of  $\text{CaCu}_3\text{Ti}_4\text{O}_{12}$  ceramics. Within the space charge model, the observed dielectric relaxation occurs when the operating parameters are set at the point where the space charge relaxation time  $\tau$  coincides with the inverse frequency  $1/2\pi f$ . In the simple space charge model of Coehlo [17, 18], the relaxation time  $\tau$  is

$$\tau = d \sqrt{\frac{\sigma}{\varepsilon D}} \quad (1)$$

where  $d$  is the thickness and  $\varepsilon$  the dielectric permittivity of the space charge material;  $\sigma$  is the conductivity and  $D$  the diffusion coefficient of the free charges which localize at interfaces. In  $\text{CaCu}_3\text{Ti}_4\text{O}_{12}$  the conducting electrons are thought to arise from incomplete compensation of Cu-related defects, the interfaces are grain boundaries and the free charges are moving inside the grains and localizing at grain boundaries. This model is supported by the similarities between the activation energies of inner grain conductivity, which is 80 meV [13], and of the dielectric relaxation, which is 90 meV [15]. Using equation (1), one can then understand why the magnetocapacitance is large at the relaxation frequency. Indeed, the applied magnetic field interacts with the mobile free charges thus tuning  $\sigma$  and  $D$  and altering  $\tau$ . As a result of this shift of  $\tau$ , the dispersion of the capacitance and that of the dielectric losses undergo a shift which is shown as derivatives in figures 2(a) and (b). Following the Debye model [17], the frequency dispersion of the capacitance is an S-shaped decrease whose derivative is a parabolic-type curve (figure 2(a)) and the frequency dispersion of the dielectric losses is a parabolic maximum whose derivative is an S-shaped curve (figure 2(b)). To further quantify this magnetic-field-induced dielectric dispersion, one should thus need the  $\tau(H)$  variation, which is not known but can be estimated. Using

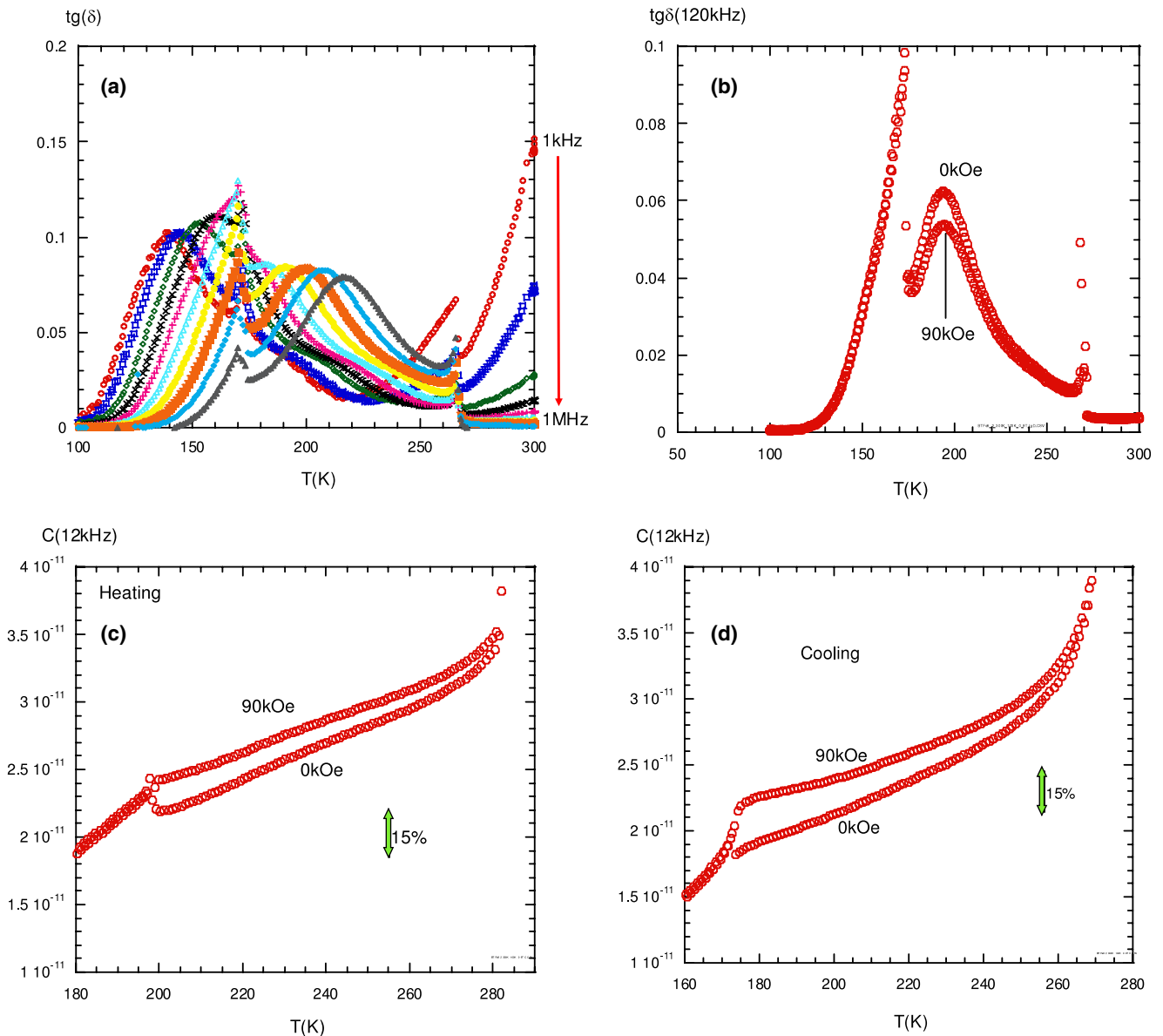


**Figure 3.** (a) Dielectric losses of a BaTiO<sub>3</sub>:Fe single crystal versus temperature for several frequencies. The two sharp anomalies at 170 and 270 K mark the ferroelectric phase transitions while the diffuse and shifted maximum stems from the relaxation of domain walls. (b) In the temperature range of the domain wall relaxation the dielectric losses are strongly depressed by a magnetic field of 90 kOe. On heating (c) and cooling (d), a 15% magnetocapacitance is observed still in the temperature range of domain wall relaxation.

the temperature variation of  $\tau$  without a magnetic field, one can compute the equivalent temperature variation that would lead to the dispersion of figure 2 and find  $\Delta T = 0.1$  K ( $\Delta\tau/\tau = 3\%$  at 110 K). We recall that the actual variations of  $T$  are less than 0.01 K over the whole temperature range and thus the effective variation of  $\tau$  should come out of the three parameters in equation (1). Since CaCu<sub>3</sub>Ti<sub>4</sub>O<sub>12</sub> is not an intrinsic magnetodielectric material the variation of  $\varepsilon$  versus  $H$  can be neglected and the whole change of  $\tau$  is to be ascribed to  $\sigma$  or  $D$ . Under the assumption of only a magnetoconduction effect, a change of  $\sigma$  of a few per cent under 90 kOe is enough to recover the observed shift of  $\tau$  and the effective dielectric tuning. There is at present no evidence for such a bulk magnetoconductivity of CaCu<sub>3</sub>Ti<sub>4</sub>O<sub>12</sub> but, because of its heterogeneity, it is a highly nonlinear

material. Within such a rough and preliminary model, it is the accumulation of free charges which is the source of our observations. Such interaction between space charges and the external magnetic field thus explains why magnetocapacitance occurs in CaCu<sub>3</sub>Ti<sub>4</sub>O<sub>12</sub> ceramics with no need for direct coupling to the dielectric permittivity. These results are in full agreement with the interface model of Catalan [8]; only the observed shift of  $\tau$  is much smaller than the computed one because, in this latter case, a large magnetoresistance of 90% was used.

The last example of interface-related magnetocapacitance will be taken within ferroelectric single crystals. Indeed, in these materials, sharp domain walls are separating macro- or micro-domains of homogeneous polarization. The dynamics of these domain walls is at the origin of the ferroelectric hysteresis

loops fully analogous to the ferromagnetic loops [19]. However, unlike ferromagnetic domain walls, ferroelectric domain walls carry a strong energy which depends on the exact crystalline symmetry of the ferroelectric phase. Because of this energy, which is of polar origin, the motion of the domain walls can have macroscopic contributions to the overall dielectric permittivity of ferroelectrics. In BaTiO<sub>3</sub>, joint elastic and dielectric experiments clearly show this dynamical contribution resulting in a relaxation with about 1 eV activation energy [20]. Moreover, the pinning of this motion by charged point defects was pointed out many times. In our present experiment, we want to take advantage of this interaction between domain wall dynamics and charged defects to induce an artificial magnetocapacitance. This is why we investigated Fe-doped BaTiO<sub>3</sub> single crystals where the charged defects originate from the heterovalent substitution of Ti<sup>4+</sup> cations by Fe<sup>3+</sup> impurities associated with charged oxygen vacancies. These crystals have been deeply investigated because of their interesting optical properties [21]. The dynamical contribution of domain walls to the dielectric properties was, however, little investigated. In figure 3(a), the dielectric loss of a BaTiO<sub>3</sub> crystal containing 0.075 at.% of Fe is plotted versus temperature between 300 and 4 K. Starting from the high temperature side, we can see two sharp and frequency-independent anomalies at about 270 and 170 K, showing the tetragonal to orthorhombic and the orthorhombic to rhombohedral phase transition, respectively. Next, a broad maximum is seen whose temperature of occurrence is shifted from 140 to 220 K as the frequency is scanned from 1 kHz to 1 MHz. This relaxation process has an activation energy of about 1 eV and it is not affected by the ferroelectric transition occurring at 170 K. Both these features are in full agreement with previous reports on undoped BaTiO<sub>3</sub> ceramics showing that it originates from domain wall motion [20]. The magnetic field influence on this relaxation is shown in figure 3(b) for a single frequency ( $f = 100$  kHz) at two similar cooling runs, one for  $H = 0$  Oe and the other for  $H = 90$  kOe (figure 3(b)). Only in the vicinity of the relaxation maximum does the dielectric loss depend on the magnetic field. The same coupling features are observed in the capacitance for cooling (figure 3(c)) and heating (figure 3(d)) runs. One can see that the 15% magnetocapacitance is restricted to the temperature ranges where domain wall relaxation occurs. If the operating frequency is changed, the occurrence of magnetocapacitance shifts following the trends of figure 3(a). Away from domain wall relaxation, no magnetocapacitance was observed. Again, the charge localization at the interface model holds for this magnetodielectric coupling. Indeed, we already stressed that the domain wall relaxation is pinned by charged defects. At the same time, the Fe-related charged defects are increasing the conductivity of these single crystals. We thus have again the two ingredients—interfaces and free charges—leading to a magnetodielectric coupling. Linking these observations with the above model drawn for CaCu<sub>3</sub>Ti<sub>4</sub>O<sub>12</sub> will require further experimental investigation. In particular, as seen in figure 3(b), the relaxation temperature is not altered by the magnetic field. This was confirmed by a full fitting of the Arrhenius law of the domain wall relaxation which shows no influence of the

magnetic field. Unlike CaCu<sub>3</sub>Ti<sub>4</sub>O<sub>12</sub>, the relaxation time is not shifted by the magnetic field while the relaxation amplitude undergoes a sizable change seen in both the dielectric losses (figure 3(b)) and the capacitance (figures 3(c) and (d)). We have thus to assume that the density and the moment of relaxing dipoles are affected by the magnetic field. Further investigations are underway to better understand this on tuning the density of domain walls and of point charges so as to tune the effective magnetocapacitance.

In all the materials that we have investigated, the localization of free charges at interfaces is the common driving source for the magnetocapacitance coupling. The free charges may be of different origins and the interfaces of different shapes and nature: however, whenever free charge localization contributes to the effective dielectric permittivity a magnetocapacitance is observed close to the space charge relaxation frequency. We thus conclude that any device including at the same time interfaces and free charges may lead to strong magnetocapacitance coupling. The observation of magnetocapacitance in ferroelectric crystals doped with heterovalent impurities may also lead to novel routes towards the coupling between an external magnetic field and ferroelectric polarization.

This work is taking place within the FAME European Network of Excellence and the STREP project MACOMUFI.

## References

- [1] Fiebig M 2005 Revival of the magnetoelectric effect *J. Phys. D: Appl. Phys.* **38** R123–52
- [2] Hill N A 2000 Why are there so few magnetic ferroelectrics? *J. Phys. Chem. B* **104** 6694–709
- [3] Kimura T, Goto T, Shintani H, Ishizuka K, Arima T and Tokura Y 2003 Magnetic control of ferroelectric polarization *Nature* **426** 55–8
- [4] Zheng H, Wang J, Lofland S E, Ma Z, Mohaddes-Ardabili L, Zhao T, Salamanca-Riba L, Shinde S R, Ogale S B, Bai F, Vielhand D, Jia Y, Schlom D G, Wuttig M, Roytburd A and Ramesh R 2004 Multiferroic BaTiO<sub>3</sub>–CoFe<sub>2</sub>O<sub>4</sub> nanostructures *Science* **303** 661–3
- [5] Shi Z, Nan C W, Zhang J, Cai N and Li J-F 2005 Magnetoelectric effect of Pb(Zr, Ti)O<sub>3</sub> rod arrays in a (Tb, Dy)Fe<sub>2</sub>/epoxy medium *Appl. Phys. Lett.* **87** 012503
- [6] Srinivasan G, De Vreugd C P, Laletin V M, Paddubnaya N, Bichurin M I, Petrov V M and Filippov D A 2005 Resonant magnetoelectric coupling in trilayers of ferromagnetic alloys and piezoelectric lead zirconate titanate: the influence of bias magnetic field *Phys. Rev. B* **71** 184423
- [7] Israel C, Mathur N D and Scott J F 2008 A one-cent room-temperature magnetoelectric sensor *Nat. Mater.* **7** 93–4
- [8] Catalan G 2006 Magnetocapacitance without magnetoelectric coupling *Appl. Phys. Lett.* **88** 102902
- [9] Ramirez A P, Subramanian M A, Gardel M, Blumberg G, Li D, Vogt T and Shapiro S M 2000 Giant dielectric constant response in a copper-titanate *Solid State Commun.* **115** 217–20
- [10] Ikeda N, Ohsumi H, Ohwada K, Ishii K, Inami T, Kakurai K, Murakami Y, Yoshii K, Mori S, Horibe Y and Kito H 2005 Ferroelectricity from iron valence ordering in the charge-frustrated system LuFe<sub>2</sub>O<sub>4</sub> *Nature* **436** 1136–8
- [11] Wu J, Nan C-W, Lin Y and Deng Y 2002 Giant dielectric permittivity observed in Li and Ti doped NiO *Phys. Rev. Lett.* **89** 217601

- [12] Raevski I P, Prosandeev S A, Bogatin A S, Malitskaya M A and Jastrabik L 2003 High dielectric permittivity in  $A\text{Fe}_{1/2}\text{B}_{1/2}\text{O}_3$  non-ferroelectric perovskite ceramics. A = Ba, Sr, Ca; B = Nb, Ta, Sb *J. Appl. Phys.* **93** 4130–6
- [13] Sinclair D C, Adams T B, Morrison F D and West A R 2002  $\text{CaCu}_3\text{Ti}_4\text{O}_{12}$ : one-step internal barrier layer capacitor *Appl. Phys. Lett.* **80** 2153–5
- [14] Subramanian M A, He T, Chen J, Rogado N S, Calvarese T G and Sleight A W 2006 Giant room-temperature magnetodielectric response in the electronic ferroelectric  $\text{LuFe}_2\text{O}_4$  *Adv. Mater.* **18** 1737–9
- [15] Maglione M 2008 *Charge Transfer and Vibronic States in Ionic–Covalent Systems. Theory, Experiment, and Applications* (*Springer Series of Topics in Solid-State Sciences*) ed V S Vikhnin and G K Liu (Berlin: Springer/Tsinghua University Press)
- [16] Sze S M and Kwok K Ng 2007 *Physics of Semiconductor Devices* 3rd edn (New York: Wiley)
- [17] *Coelho Physics of Dielectrics* 1978 (Amsterdam: Elsevier)
- [18] Bidault O, Goux P, Kchikech M, Belkaoumi M and Maglione M 1994 Space charge relaxation in perovskites *Phys. Rev. B* **49** 7868–73
- [19] Lines M E and Glass A M 1979 *Principles and Applications of Ferroelectrics and Related Materials* (Oxford: Clarendon)
- [20] Cheng B L, Gabbay M, Maglione M and Fantozzi G 2003 Relaxation motion and possible memory of domain structures in barium titanate ceramics studied by mechanical and dielectric loss *J. Electroceram.* **10** 5–18
- [21] Godefroy G and Perrot A 1984 Dielectric relaxation in Fe or Nb doped barium titanate single crystals *Ferroelectrics* **54** 87–90